frontiers | Frontiers in Cardiovascular Medicine

TYPE Original Research
PUBLISHED 21 July 2025
DOI 10.3389/fcvm.2025.1586775



OPEN ACCESS

EDITED BY
Olivier M. Vanakker,
Ghent University, Belgium

REVIEWED BY
Yuhua Wei,
University of Alabama at Birmingham, United States
Ningjing Qian,
Zhejiang University, China

*CORRESPONDENCE
Q. Tang
✉ qtang@ed.ac.uk
V. E. MacRae
✉ vicky.macrae@roslin.ed.ac.uk

†These authors have contributed equally to this work

RECEIVED 03 March 2025
ACCEPTED 04 July 2025
PUBLISHED 21 July 2025

CITATION
Phadwal K, Tang Q, Kurian D, Tan X, Cawthorn WP and MacRae VE (2025) Nutrient restriction protects against valve interstitial cell calcification by upregulating ubiquitin mediated proteolysis.
Front. Cardiovasc. Med. 12:1586775.
doi: 10.3389/fcvm.2025.1586775



# Nutrient restriction protects against valve interstitial cell calcification by upregulating ubiquitin mediated proteolysis

K. Phadwal[1†], Q. Tang[1*†], D. Kurian[1], X Tan[1], W. P. Cawthorn[2] and V. E. MacRae[1,3*]

[1]The Roslin Institute and Royal (Dick) School of Veterinary Studies, University of Edinburgh, Midlothian, United Kingdom, [2]University/BHF Centre for Cardiovascular Science, The Queen's Medical Research Institute, Edinburgh Bioquarter, University of Edinburgh, Edinburgh, United Kingdom, [3]School of Life Sciences, Faculty of Science and Engineering, Anglia Ruskin University, Cambridge, United Kingdom

**Introduction:** Calcific aortic valve disease (CAVD) is a common and progressive valvular heart disease characterised by the pathological calcification of valve interstitial cells (VICs). Current clinical treatments, such as surgical valve replacement and transcatheter valve implantation, are invasive and do not target the underlying molecular mechanisms of calcification. Emerging evidence suggests that metabolic interventions may modulate cellular calcification processes. In this study, we investigated the potential of nutrient restriction (NR) as a non-invasive strategy to mitigate VIC calcification, with a particular focus on the role of the ubiquitin-proteasome system (UPS).

**Methods:** Primary rat valvular interstitial cells (RVICs) were cultured and subjected to in vitro calcification using calcium- and phosphate-enriched media. Nutrient restriction was induced by incubating cells in Hank's Balanced Salt Solution (HBSS). Calcification was assessed by quantifying calcium deposition and osteogenic marker expression. To explore the underlying molecular changes, a stable isotope labelling by amino acids in cell culture (SILAC)-based proteomic analysis was performed. The role of the UPS was further examined using pharmacological inhibition with MG132 and siRNA-mediated knockdown of key UPS components, including Cullin-2 (Cul2) and Ubiquitin-conjugating enzyme E2 H (Ube2H).

**Results:** Nutrient restriction significantly downregulated the expression of osteogenic markers and reduced calcium deposition in RVICs. SILAC-based proteomics revealed the upregulation of multiple components of the UPS in nutrient-restricted cells. Notably, Cul2 and Ube2H were identified as potential key mediators of the anti-calcification effects observed. Inhibition of the proteasome with MG132 exacerbated calcification, while knockdown of Cul2 using siRNA increased osteogenic marker expression and calcium deposition, indicating the essential role of Cul2 in modulating VIC calcification under nutrient-restricted conditions.

**Conclusion:** This study demonstrates that nutrient restriction effectively attenuates VIC calcification through the modulation of the ubiquitin-proteasome system. The protective role of UPS components, particularly Cul2 and Ube2H, suggests that targeting this pathway could represent a novel therapeutic approach for the management of CAVD. These findings also raise the possibility of employing dietary or metabolic interventions as non-invasive strategies to prevent or delay valve calcification.

KEYWORDS

**nutrient restriction, calcific aortic valve disease, ubiquitin mediated proteolysis, Cullin-2, SILAC**

# Introduction

Aortic stenosis (AS) is the most prevalent valvular heart disease, with a reported prevalence of 10% for severe AS in adults aged 80 years and older (1). Degenerative calcific aortic valve disease (CAVD), predominantly age-related, constitutes the most common etiology of AS in the elderly, affecting over 25% of individuals over 65 years of age (2). The pathophysiology of CAVD shares significant parallels with physiological bone mineralization. Valvular interstitial cells (VICs), the predominant cell type within the aortic valve, play a central role in the progression of CAVD. Prior research has demonstrated that VICs can undergo osteogenic differentiation, acquiring a bone-like phenotype accompanied by increased protein expression of osteogenic markers such as RUNX family transcription factor 2 (RUNX2) (3), osteocalcin (OCN) (4), bone sialoprotein (BSP) (5) and osterix (6).

Current treatment options for CAVD primarily involve surgical valve replacement or transcatheter aortic valve implantation (TAVI) with prosthetic valves (7). However, these interventions are invasive and carry high risks. Additionally, prosthetic valves have limited durability, ultimately succumbing to structural degeneration and calcification. Therapeutic strategies targeting aging or extending healthspan are notably absent from the current standard of care for CAVD. While lifestyle modifications, including smoking cessation and increased physical activity, have been integrated into the management of cardiovascular risk factors, these interventions do not directly address the aging process itself. Notably, over a century of aging research has identified dietary interventions as among the most effective approaches for extending lifespan and healthspan across various organisms (8). Nutritional strategies aimed at healthspan extension therefore represent a promising avenue for addressing CAVD without introducing adverse effects.

NR, including regimens such as fasting or ketogenic diets, holds considerable potential for exerting protective cardiovascular effects (9). While NR protocols vary widely—ranging from time-restricted feeding to prolonged fasting or diets restricted in specific nutrients—several common systemic responses to NR have been observed. These include reductions in circulating levels of glucose, insulin, insulin-like growth factor 1 (IGF-1), growth hormone, leptin and adrenaline, alongside increases in ketone bodies, IGF-binding protein 1 (IGFBP1), fibroblast growth factor 21 (FGF21), cortisol, adiponectin and glucagon (10). At the cellular level, NR suppresses growth pathways such as mechanistic target of rapamycin (mTOR) and mitogen-activated protein kinases (MAPK), activates the master energy sensor AMP-activated protein kinase (AMPK), and induces autophagy (11, 12). In the present study, we demonstrate, for the first time, the potential of nutrient restriction (NR) to mitigate calcification in VICs, thereby highlighting NR as a promising non-invasive intervention for preventing VIC calcification.

# Materials and methods

## RVIC culture and calcification

Rat valvular interstitial cells (RVICs) were cultured in DMEM/F-12 growth medium (Gibco), supplemented with 10% fetal bovine serum (FBS) and 1% gentamycin (Gibco), and seeded in 12-well plates at a density of $3 \times 10^4$ cells per well. Calcification was induced as previously described (13). Cells were maintained until they reached 70%–80% confluence, at which point they were exposed to either control medium supplemented with 1.05 mM calcium (Ca) and 0.95 mM phosphate (Pi) or calcifying media containing 2.5 mM Ca and 2.7 mM Pi. Cultures were incubated for up to 72 h in a humidified environment at 5% $CO_2$.

## *In vitro* nutrient deprivation

To induce nutrient deprivation, cultured cells were maintained in DMEM/F-12 growth medium (Gibco) until they reached the desired confluence (typically 70%–80%). Subsequently, the growth medium was aspirated, and the cells were gently rinsed with pre-warmed phosphate-buffered saline (PBS) to remove residual nutrients. The cells were then incubated in Hank's Balanced Salt Solution (HBSS), supplemented with 2.5 mM calcium (Ca) and 2.7 mM phosphate (Pi), at 37°C in a humidified atmosphere containing 5% $CO_2$ for 24–48 h. Following the nutrient deprivation period, the HBSS was replaced with appropriate culture medium for downstream treatments or experimental analysis.

## Cell viability assay

Cells were seeded into a microplate at a density of $3 \times 10^4$ cells per well and allowed to adhere overnight. Subsequently, the Alamar Blue reagent was added to the culture medium at a concentration constituting 10% of the total volume, as previously described (14). The plate was incubated at 37°C in a humidified atmosphere with 5% $CO_2$ for up to 4 h, during which metabolically active cells reduced the reagent, resulting in a detectable colorimetric change. Absorbance was measured at wavelengths of 570 nm and 600 nm. The results were then analyzed to assess cell viability across samples, with the degree of reagent reduction serving as an indicator of metabolic activity.

## MG132 treatment

To induce UPS inhibition, cultured cells were maintained in DMEM/F-12 growth medium (Gibco) until they reached the desired confluence (typically 70%–80%). The cells were then incubated with the 20S proteosome inhibitor MG132 (Cayman) for 48 h (50 or 100 nm), supplemented with 2.5 mM Ca and

2.7 mM Pi, at 37°C in a humidified atmosphere containing 5% $CO_2$. Following MG132 treatment, cells were collected for further experimental analysis.

## Alizarin red staining

Cells were cultured in plates and subjected to calcification treatment as previously described (13). After removing the culture medium, the cell monolayer was gently rinsed with PBS and fixed in 10% neutral-buffered formalin (NBF) for 15 min at room temperature (RT). Following fixation, the cells were washed twice with PBS to remove residual fixative. The monolayer was then stained with 2% Alizarin S solution (pH 4.2, 500 µl per well) for 10 min at RT to detect calcium deposition. Excess staining solution was discarded, and the cells were washed thoroughly three times with distilled water to remove unbound dye. The plates were allowed to air-dry completely before imaging.

## Calcium assay

Calcium deposition was quantified according to the established protocol (13). Briefly, RVICs were washed with PBS and subsequently incubated in 0.6 N hydrochloric acid (HCl) at 4°C for 24 h to solubilize deposited calcium. The liberated calcium was quantified colorimetrically using a commercially available assay kit based on its stable interaction with σ-Cresolphthalein (Randox Laboratories). The measured calcium content was subsequently normalized to the total protein concentration of each sample, determined using the DC protein assay (Bio-Rad Laboratories).

## RNA interference (RNAi) treatment

RVICs at approximately 70% confluence were utilized for siRNA transfection studies following an established protocol (15). For each transfection, 6 µl (60 ρM) siRNA targeting Cul2 (Santa Cruz) or non-targeting scrambled control (SC) siRNA (Santa Cruz) was used. The cells were incubated at 37°C in Opti-MEM medium (Gibco) containing the respective siRNA and Lipofectamine 3,000 (Thermo Fisher) for up to 7 h. Subsequently, the transfection medium was replaced with complete growth medium, and the cells were cultured for an additional 72 h to facilitate siRNA-mediated gene silencing. Following this period, the transfected RVICs were cultured for 24 h in either DMEM or HBSS, both supplemented with 2.7 mM calcium and 2.5 mM phosphate. Subsequently, the cells were collected for downstream analyses.

## SILAC labelling and quantitative proteomics of RVICs

RVICs were cultured over six passages in either "light" DMEM/F-12 R0K0 medium (DC Biosciences, LM038) or "heavy" DMEM/F-12 R10K8 medium (DC Biosciences, LM040), as previously described (16). Both media were supplemented with SILAC-dialyzed FBS (DC Biosciences, DS1002) to ensure proper isotopic labelling. Following the sixth passage, RVICs labelled with "light" isotopes were cultured in DMEM supplemented with calcium and phosphate (DMEM-CaPi), while RVICs labelled with "heavy" isotopes were incubated in HBSS with calcium and phosphate (HBSS-CaPi) for 24 h. After treatment, cells were trypsinized, and cell pellets were washed twice with cold PBS prior to sample preparation for quantitative mass spectrometry (MS).

Cell pellets were resuspended in 10% trifluoroethanol (pH 8.0) and subjected to gentle vortexing for 1 h to ensure solubilization. Proteins were reduced with 5 mM dithiothreitol (DTT) and alkylated with 10 mM iodoacetamide before digestion with sequencing-grade modified trypsin (Promega). The resulting peptide mixtures were centrifuged at 800 × g to pellet any insoluble material, and the supernatant containing digested peptides was collected. The peptides were cleaned using StageTips to remove impurities.

Quantitative proteomics was performed using nanoflow liquid chromatography-tandem mass spectrometry (nanoLC-MS/MS) on a micrOTOF-II mass spectrometer (Bruker, Germany) coupled to an RSLCnano LC system (Thermo). Tryptic peptides were first delivered to a trap column at a flow rate of 20 µl/min with 100% solvent A (0.1% formic acid in LC-MS grade water) for 4 min of loading and washing. Peptides were then transferred to an analytical column and separated at 300 nl/min using a 60-min gradient from 7% to 35% solvent B (0.1% formic acid in acetonitrile). Eluted peptides were electrosprayed directly into the mass spectrometer for MS and MS/MS analysis in a data-dependent acquisition mode. MS scans were performed over the m/z range of 300–2,000, followed by MS/MS scans of the six most intense ions. Rolling collision energy was applied for fragmentation based on precursor ion mass, and dynamic exclusion was set at 30 s to avoid repeated fragmentation of the same ions.

Raw spectral data were processed using DataAnalysis software (Bruker), and imported into ProteinScape 3.1 server (Bruker), where the spectral data were searched against the Uniprot rat sequence database (containing 22,367 entries) using Mascot 2.4 (Matrix Science). Search parameters included a peptide precursor ion mass tolerance of 25 ppm and a fragment ion mass tolerance of 0.05 Da. Peptide charge states were set to 2+ and 3+, with carbamidomethylation of cysteine as a fixed modification and oxidation of methionine, Label:13C(6)15N(4) of Arginine and Label:13C(6)15N(2) of Lysine, as variable modifications. Peptide identifications were filtered to achieve a false discovery rate (FDR) of <1% by incorporating a decoy database search. SILAC quantification was performed by using WARPLC plugin on Proteinscape 3.1 software to integrate extracted ion chromatogram of every precursor. Peptide ratios were normalized based on setting overall peptide median ratio at one, which corrects for unequal protein sampling and a coefficient of variability of peptide ratios were also determined for each quantified protein.

## Immunoblotting

Immunoblotting was performed as previously reported (17, 18). Protein lysates were prepared using radioimmunoprecipitation assay (RIPA) buffer supplemented with the Halt Protease Inhibitor Cocktail (Thermo Fisher Scientific). The protein concentration of the lysates was quantified using the Pierce BCA Protein Assay Kit (Thermo Fisher Scientific). Samples were mixed with 4× loading buffer, boiled and resolved on a 4%–12% Bis-Tris gel (Invitrogen) via sodium dodecyl sulfate–polyacrylamide gel electrophoresis (SDS-PAGE). Proteins were subsequently transferred onto polyvinylidene difluoride (PVDF) membranes (Thermo Fisher Scientific). Membranes were blocked for 1 h using 5% skimmed milk in phosphate-buffered saline with 0.1% Tween-20 (PBST) and incubated overnight at 4°C with primary antibodies diluted 1:1000 in 5% skimmed milk. Primary antibodies included those against Runx2 (Abcam, ab236639), Cul2 (Proteintech, 10981-2-AP), Ube2h (Proteintech, 15685-1-AP), OCN (Proteintech, 23418-1-AP), Osterix (Proteintech, 28694-1-AP), β-actin (Proteintech, 66009-1-Ig) and bone sialoprotein (Invitrogen, PA5-79425). Following washing, membranes were incubated for 1 h with secondary antibodies. Horseradish peroxidase (HRP)-conjugated goat anti-rabbit IgG (Dako, P0449) was employed. Blots were then visualized using the GeneGnome imaging system (Syngene).

## ATP measurement

Intracellular ATP levels were measured using a commericial ATP Assay Kit (ab83355, Abcam) according to the manufacturer's instructions. Briefly, cells were washed with cold PBS, lysed in ATP Assay Buffer, and centrifuged at 13,000 × g for 5 min at 4°C to remove insoluble material. Supernatants were collected and incubated with the ATP reaction mix containing ATP Converter, Developer, and ATP Probe in a 1:1 ratio. After 30 min of incubation at room temperature in the dark, the signal was measured using a microplate reader at 570 nm (colorimetric). ATP concentrations were calculated based on a standard curve generated using known concentrations of ATP.

## Statistical analysis

All data are presented as the mean ± standard error of the mean (SEM). Statistical analyses were performed using either a paired *t*-test or one-way analysis of variance (ANOVA) followed by Tukey's *post hoc* test, depending on the experimental design. All computations were conducted with GraphPad Prism software, and statistical significance was defined as a *p*-value less than 0.05. Significance levels were indicated as follows: $*p < 0.05$, $**p < 0.01$, and $***p < 0.001$. The sample size (N) corresponds to the number of independent cultures evaluated.

# Results

## Nutrient deprivation inhibits calcification in RVICS

To assess the impact of NR on RVIC calcification, calcification was evaluated in RVICs cultured in either complete DMEM media or HBSS, an established model of nutrient deprivation (19), in the presence of 2.7 mM Ca and 2.5 mM Pi. Nutrient deprivation significantly attenuated calcification in RVICs, as demonstrated by reduced alizarin red staining and diminished calcium deposition (Figures 1A,B). Cell viability assessment revealed that RVICs displayed enhanced viability after 48 h of HBSS treatment (Figure 1C). Consistently, intracellular ATP levels were elevated in the HBSS-treated group compared to the calcified group, further supporting the observation of enhanced metabolic activity (Figure 1D). Additionally, nutrient deprivation resulted in a marked downregulation of osteogenic marker protein expression in RVICs, including RUNX2, osterix, BSP and OCN (Figures 1E–J). Together these findings demonstrate that nutrient deprivation effectively reduces calcification in RVICs.

## Ubiquitin proteasome pathway is enriched in nutrient-deprived RVICs

To further investigate the mechanisms by which nutrient deprivation attenuates calcification, RVICs were cultured for six passages in DMEM R0K0 and DMEM R10K8 SILAC media, followed by a 24 h calcification period in either DMEM or HBSS supplemented with 2.7 mM $Ca^{2}$? and 2.5 mM Pi. The cells were subsequently harvested for protein extraction and analyzed using LC-MS/MS (Figure 2A). Integrated ingenuity pathway analysis (IPA) of the proteomic data revealed that, compared to calcification in DMEM, calcification in HBSS enriched the protein ubiquitination pathway, nucleotide excision repair (NER) pathway, and eukaryotic initiation factor 2 (EIF2) signaling across the three experimental samples (Figures 2B,C). Notably, the most significant changes were observed in the protein ubiquitination pathway. These data suggest that the protein ubiquitination pathway represents a novel potential mechanism through which Nutrient deprivation mitigates RVIC calcification.

## Cul2 and Ube2H are increased in nutrient-deprived RVICs

To further investigate the roles of key proteins within the protein ubiquitination pathway, differentially expressed proteins (DEPs) exhibiting a fold change >1.5 in the HBSS-treated vs. DMEM-treated cells were identified (Figure 3A). Among these, Cul2 and Ube2H displayed the highest fold changes. Predicted protein-protein interactions within the ubiquitination pathway are illustrated in Figure 3B. Consistent with these findings, the upregulation of Cul2 and Ube2H at the protein level was

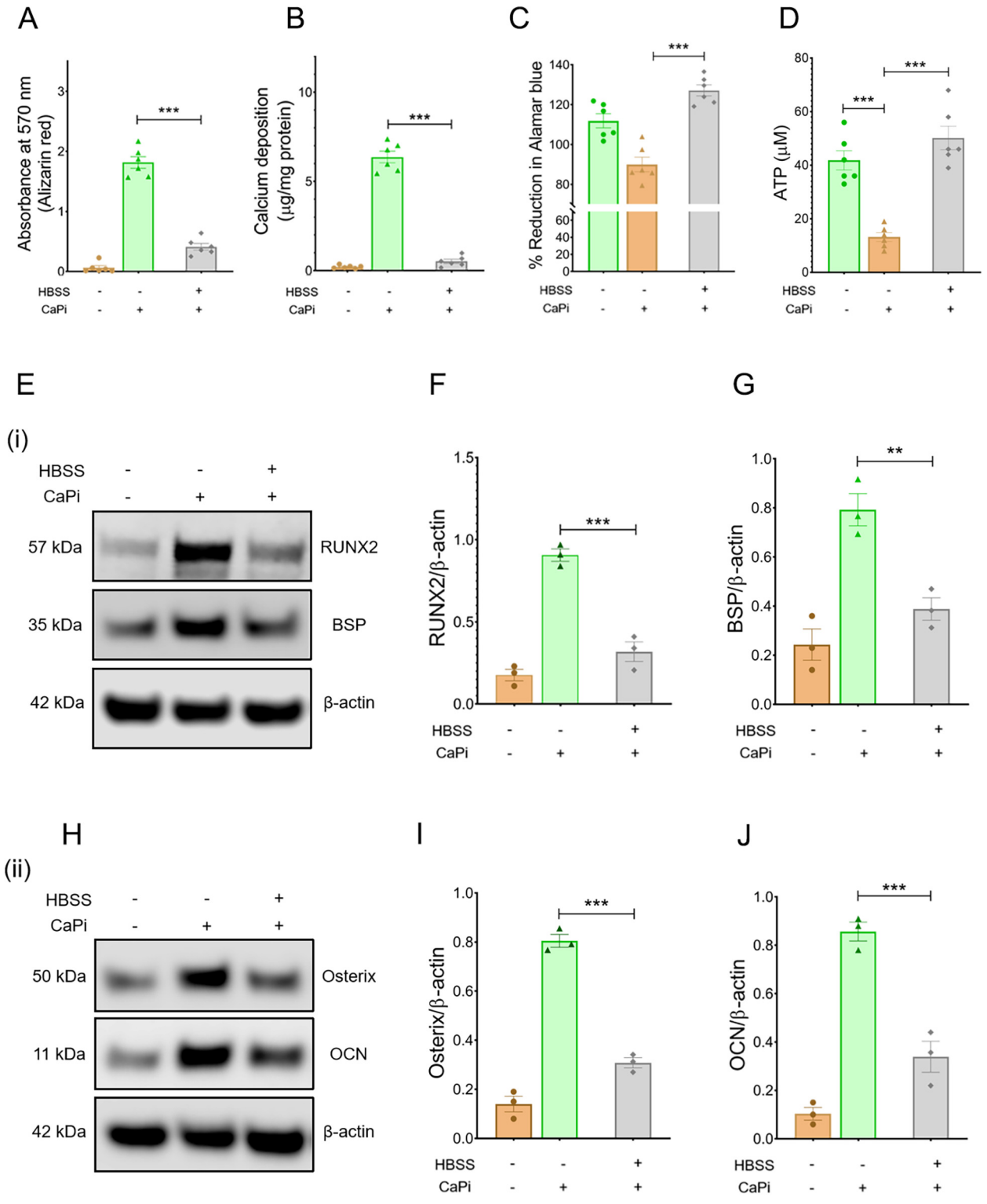


FIGURE 1
Calcification is reduced in nutrient-starved RVICS. **(A)** Quantification of alizarin red staining for RVICs cultured either with complete DMEM media or HBSS supplemented with or without 2.7Ca/2.5Pi for 48 h ($N = 6$). **(B)** Quantification of calcium deposition in RVICs cultured with complete DMEM media or HBSS in the presence of 2.7Ca/2.5Pi for 48 h ($n = 6$). **(C)** Cell viability of RVICs cultured in complete DMEM media in the presence or absence of 2.7Ca/2.5Pi and HBSS in the presence of 2.7Ca/2.5Pi for 48 h using the Alamar blue assay ($n = 6$). **(D)** ATP measurement of RVICs cultured with or without complete DMEM media in the presence or absence of 2.7Ca/2.5Pi and HBSS in the presence of 2.7Ca/2.5Pi for 48 h using the Alamar blue assay ($n = 6$). **(E)** Representative images of immunoblots for RUNX2, BSP and β-actin in RVICs cultured with or without complete DMEM media or HBSS supplemented with 2.7Ca/2.5Pi for 48 h. **(F,G)** The graphs show the ratios of RUNX2 and BSP to β-actin. **(H)** Representative images of immunoblots for osterix, OCN and β-actin in RVICs cultured with or without complete DMEM media or HBSS supplemented with 2.7Ca/2.5Pi for 48 h. **(I,J)** The graphs show the ratios of osterix and OCN to β-actin. Equal amounts of total protein were loaded in each lane, and all blots were processed in parallel under identical experimental conditions to ensure comparability. $*p < 0.05$, $**p < 0.01$, $***p < 0.001$.

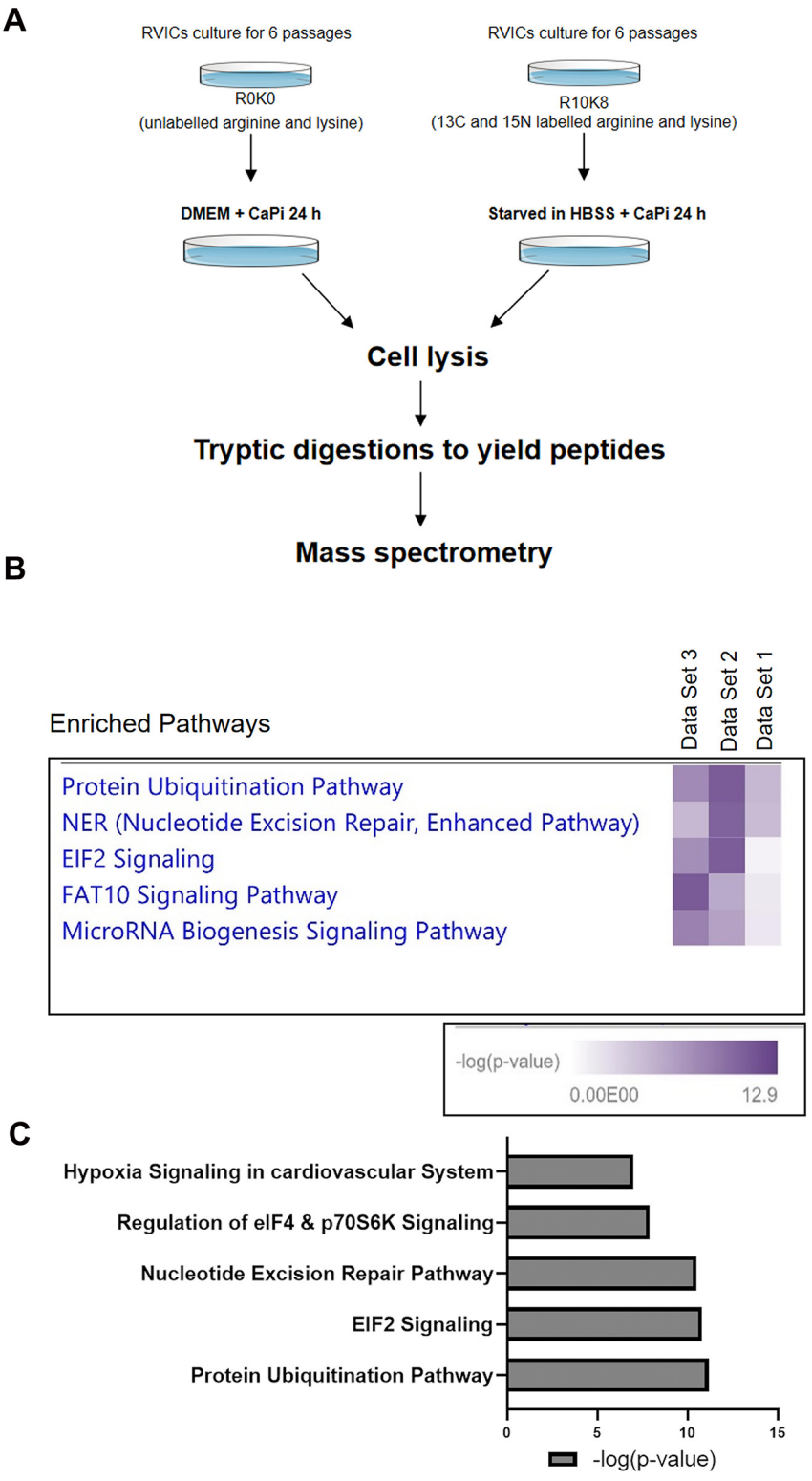


FIGURE 2
Proteomic analysis of RVICs cultured in DMEM media or HBSS supplemented with 2.7Ca/2.5Pi. **(A)** Schematic diagram of the experimental design. **(B)** Combined IPA analysis of MS shows enrichment of protein ubiquitination pathway in all three of the independent data sets ($n = 3$). **(C)** Representative graph shows enrichment of protein ubiquitination pathway with HBSS treatment, as indicated by the mean -log10($P$) value derived from three independent datasets.

**A**

| Protein ID | Fold change | Function |
|---|---|---|
| Cullin2 | 6.05 | Mediates the ubiquitination of target proteins |
| Ube2h | 2.44 | Targets abnormal or short-lived proteins for degradation. |
| Uba7 | 2.40 | Targets abnormal or short-lived proteins for degradation. |
| Skp1 | 1.95 | Essential component of the SCF (SKP1-CUL1-F-box protein) ubiquitin ligase complex, which mediates the ubiquitination of proteins. |
| Uba6 | 1.66 | Activates ubiquitin |
| Uba3 | 1.65 | Targets abnormal or short-lived proteins for degradation |

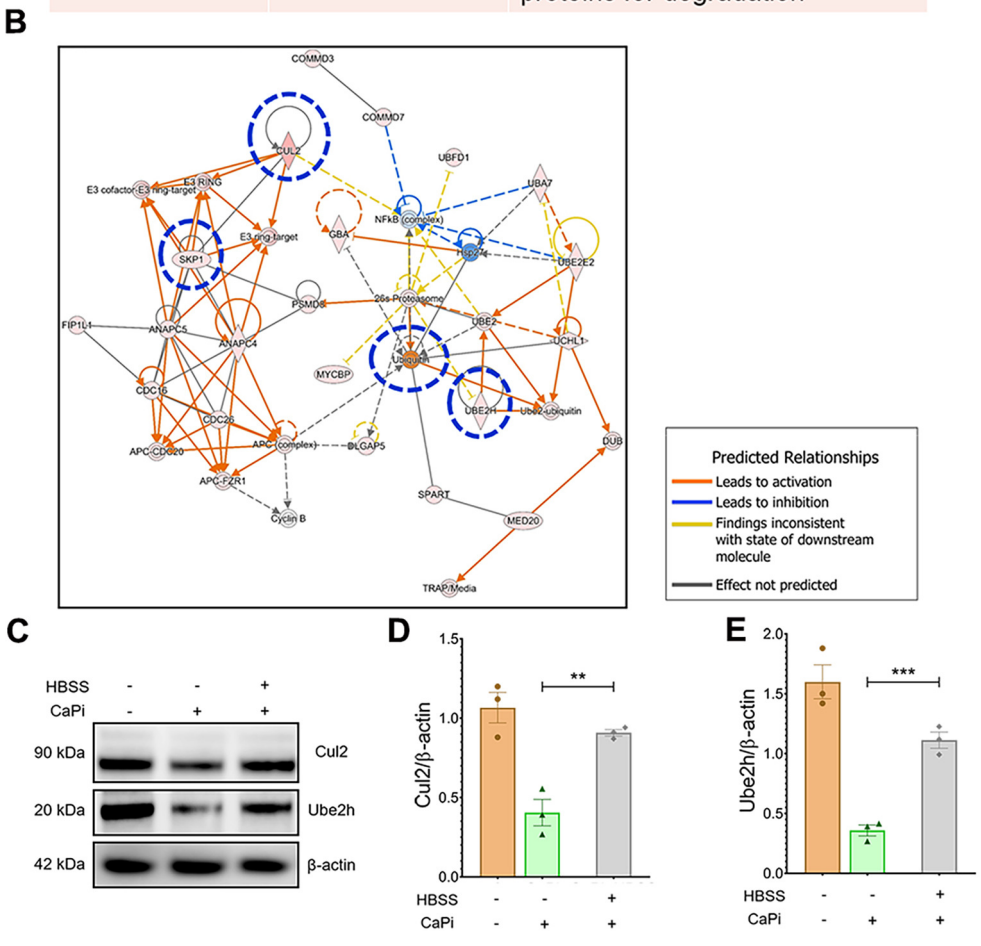


FIGURE 3
Proteomic analysis shows the upregulated UPS proteins in nutrient-deprived RVICs. **(A)** Fold change and function of proteins involved in ubiquitin proteasome pathway. **(B)** IPA network analysis shows altered activation of key UPS pathway proteins including Cul2, Ube2H, SKP1 and Ubiquitin highlighted in blue circle. Functional interconnections between the proteins are shown by arrows and lines. The blue lines represent direct associations with Annexin VI. Dashed lines represent predicted associations. **(C–E)** Validation and quantification of Cul2 and Ube2h expression by immunoblots. Equal amounts of total protein were loaded in each lane, and all blots were processed in parallel under identical experimental conditions to ensure comparability. $*p < 0.05$, $**p < 0.01$, $***p < 0.001$.

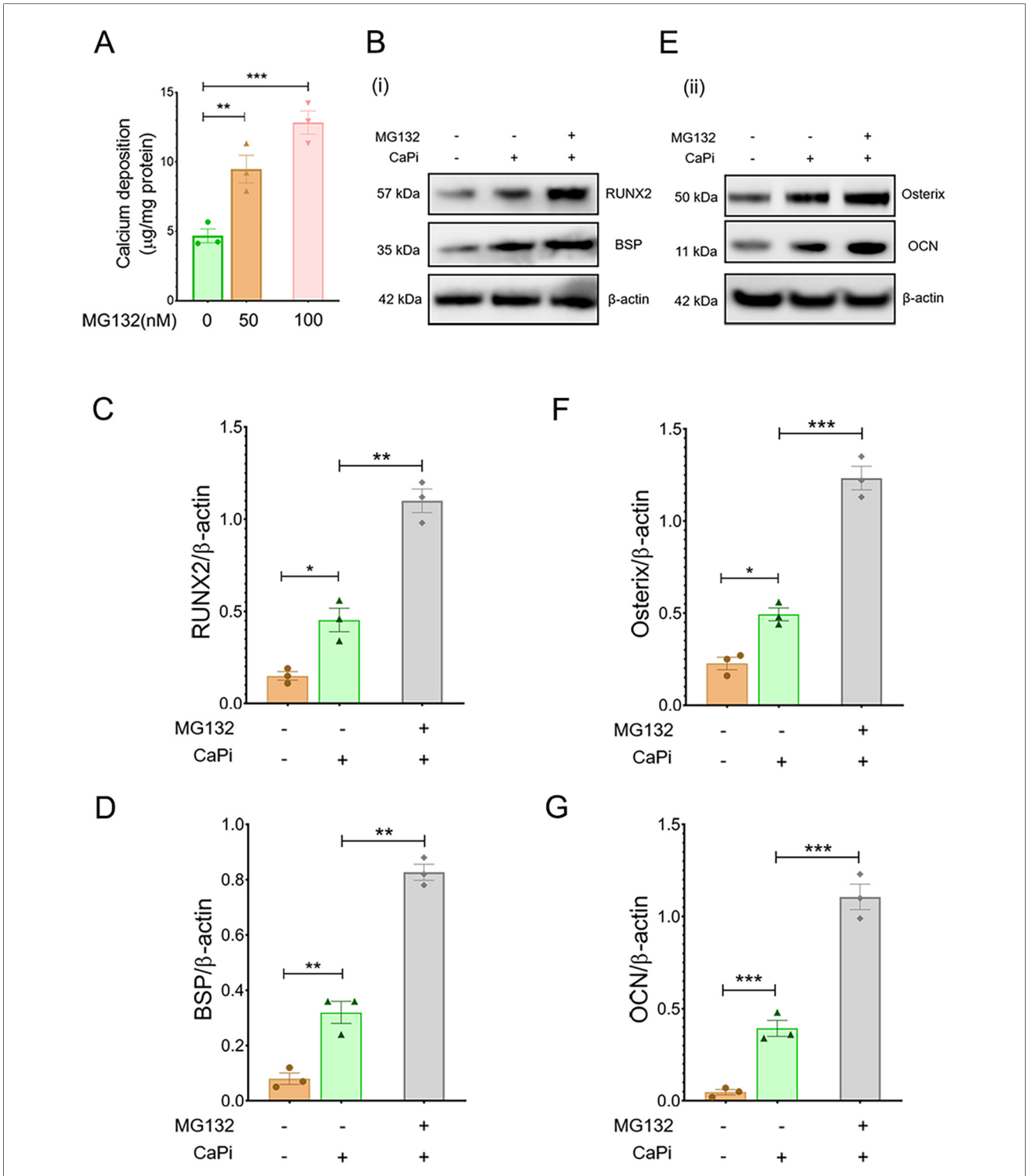


FIGURE 4
Pharmacological inhibition of Cul2 increases calcification in RVICS. **(A)** Quantification of calcium deposition in RVICs treated with 50 nM or 100 nM MG132 in complete DMEM media supplemented with 2.7Ca/2.5Pi for 48 h ($n = 3$). **(B)** Representative images of immunoblots for RUNX2, BSP and β-actin in RVICs cultured with or without 2.7Ca/2.5Pi supplemented DMEM media in the presence or absence of 100 nM MG132 for 48 h ($n = 3$). **(C,D)** The graphs show the ratios of RUNX2 and BSP to β-actin. **(E)** Representative images of immunoblots for osterix, OCN and β-actin in RVICs cultured with or without 2.7Ca/2.5Pi supplemented DMEM media in the presence or absence of 100 nM MG132 for 48 h ($n = 3$). **(F,G)** The graphs show the ratios of osterix and OCN to β-actin. Equal amounts of total protein were loaded in each lane, and all blots were processed in parallel under identical experimental conditions to ensure comparability. $^{*}p < 0.05$, $^{**}p < 0.01$, $^{***}p < 0.001$.

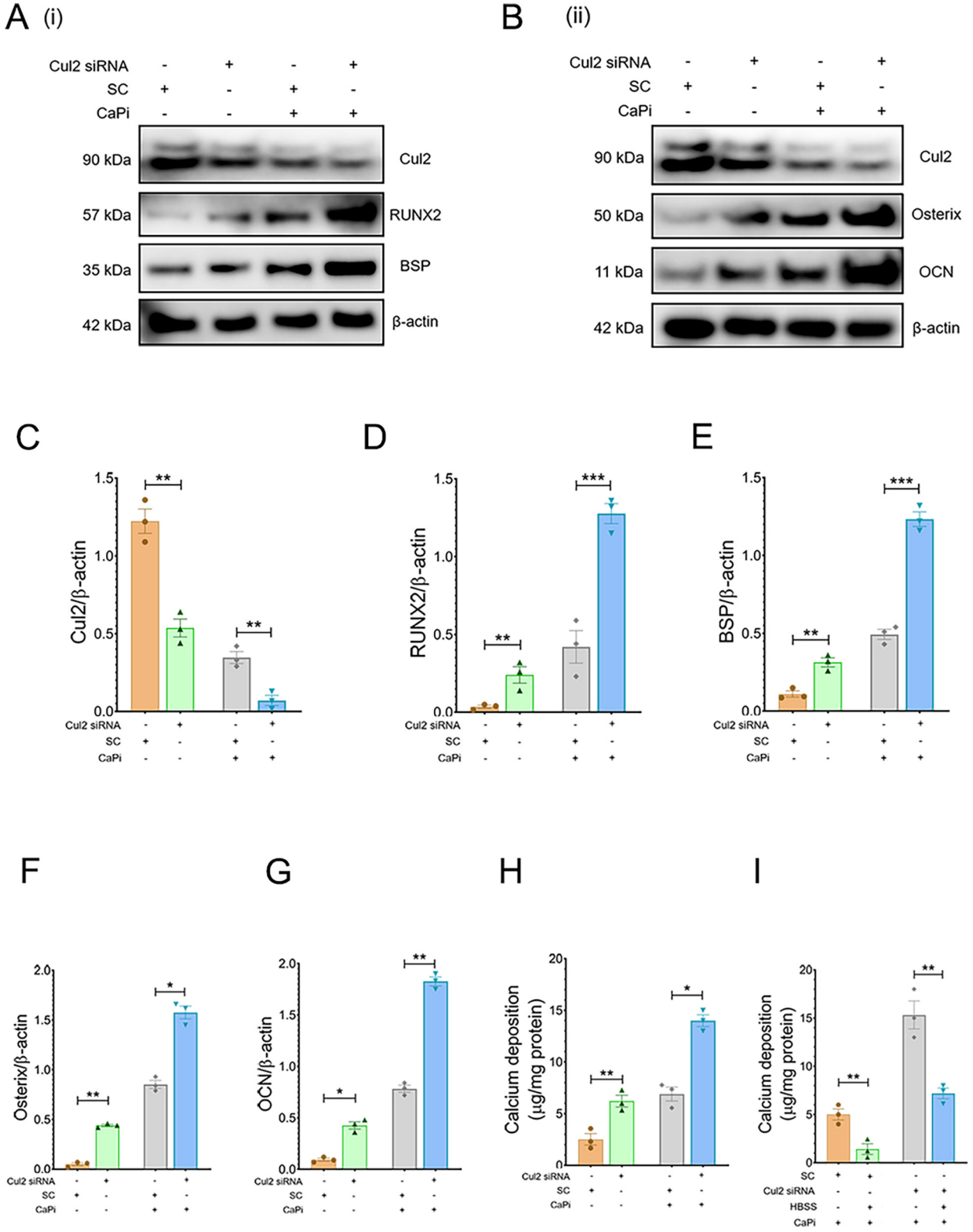


FIGURE 5
Cul2 knockdown increases calcification in RVICS. **(A,B)** Representative images of immunoblots for RUNX2, osterix, BSP, OCN and β-actin in RVICs transfected with either scrambled control (SC) or Cul2 siRNA for 72 h ($n = 3$) in the presence or abcense of 2.7Ca/2.5Pi. **(C–G)** The graphs show the ratios of Cul2, RUNX2, osterix, BSP and OCN to β-actin. Equal amounts of total protein were loaded in each lane, and all blots were processed in parallel under identical experimental conditions to ensure comparability. **(H)** Quantification of calcium deposition in RVICs transfected with either SC or Cul2 siRNA in the presence or absence of 2.7Ca/2.5Pi for 72 h ($n = 3$). **(I)** Quantification of calcium deposition in RVICs transfected with either SC or Cul2 siRNA for 72 h in 2.7Ca/2.5Pi supplemented DMEM media or HBSS. $^{*}p < 0.05$, $^{**}p < 0.01$, $^{***}p < 0.001$.

validated by immunoblotting (Figures 3C–E). Collectively, these results indicate that Cul2 and Ube2H may play pivotal roles in the protein ubiquitination pathway in nutrient-deprived RVICs.

## UPS inhibition enhances calcification in RVICS

To further assess the role of the ubiquitination pathway in regulating RVIC calcification, RVICs were exposed to MG132, a selective inhibitor of the 20S proteasome. Treatment with MG132 markedly enhanced calcium deposition (Figure 4A) and upregulated the protein expression of osteogenic markers, including RUNX2, osterix, BSP and OCN, in calcified RVICs (Figures 4B–G). Consistent with these findings, silencing Cul2, a key regulator of UPS (20), resulted in increased osteogenic transdifferentiation under both calcifying and non-calcifying conditions, as evidenced by elevated levels of RUNX2, osterix, BSP and OCN (Figures 5A–G) alongside elevated calcium deposition (Figure 5H). However, HBSS treatment alleviated calcification in RVICs both in the presence and absence of Cul2 knockdown (Figure 5I). Collectively, these results indicate that the protein ubiquitination pathway plays a critical regulatory role in RVIC calcification.

# Discussion

CAVD is the most common valvular heart disease worldwide (2). However, there are not presently any pharmaceutical treatments available to impair its progression. NR is therefore an appealing alternative to drug development or repurposing approaches. With growing evidence suggesting widespread beneficial health benefits of NR, this offers an exciting therapeutic option for CAVD. Our data support and extend a body of work proposing that NR can improve metabolic parameters, reduce cardiovascular risk factors and potentially delay the onset of age-related diseases (21). In this study we show for the first time that nutrient deprivation through treatment with HBSS significantly attenuates calcification in VICs. This observation aligns with recent research in hepatocellular carcinoma cells, whereby HBSS-induced *in vitro* nutrient deprivation enhanced the therapeutic response of the targeted cancer drug sorafenib (22).

To investigate the molecular adaptations of calcifying VICs under NR, a comprehensive SILAC analysis was performed. Our analysis revealed a pronounced upregulation of the protein ubiquitination pathway following HBSS treatment, consistent with previous findings suggesting that NR exerts cardioprotective effects through the UPS (23). This is further supported by *in vitro* studies showing that amino acid deprivation activates the UPS in human lung adenocarcinoma epithelial cells (24), as well as mechanistic studies in yeast, which revealed that NR can preserve UPS activity in aged cells (26). Our findings further demonstrate, for the first time, that treatment with MG132, an established proteasome inhibitor (25, 26), exacerbates VIC calcification, thereby highlighting the protective role of protein ubiquitination in mitigating calcification.

Ubiquitination, a highly conserved post-translational modification, involves a three-step enzymatic process mediated by E1 ubiquitin-activating enzymes, E2 ubiquitin-conjugating enzymes and E3 ubiquitin ligases, culminating in the covalent attachment of ubiquitin to substrate proteins (27). Indeed, the UPS system has been recently highlighted as a key contributor to lifespan (28). In the present study, SILAC analysis identified the upregulation of ubiquitin-activating enzymes Uba3, Uba6 and Uba7 in HBSS-treated calcifying VICs. These enzymes are known to activate ubiquitin-like modifiers, including NEDD8 (29), SUMO (30) and ISG15 (31). Indeed, NEDD8 modification and SUMOylation have been recognized as critical regulators of arterial calcification (32, 33). Moreover, we observed increased protein expression levels of Ube2h, an E2 enzyme implicated in the NEDD8 conjugation pathway, further highlighting the significance of ubiquitin-like modifiers in calcification regulation (34). Together these novel findings suggest that ubiquitin-like modifiers could serve as promising therapeutic targets for both arterial and valvular calcification, warranting further investigation to explore their potential clinical application.

Our SILAC analysis revealed a significant upregulation of Cul2 protein levels in calcifying VICs treated with HBSS. Cul2, a member of the Cullin protein family, functions as a scaffold protein that assembles with Elongin B, Elongin C, Rbx1 and various substrate recognition receptors to form Cullin-RING E3 ubiquitin ligase complexes. These complexes play a pivotal role in targeting cellular proteins for ubiquitination-mediated degradation via the 26S proteasome (35). We subsequently employed siRNA-mediated knockdown of Cul2 to investigate the impact of the destabilization of the Cullin-RING E3 ubiquitin ligase complex on VIC calcification and. Notably, Cul2 silencing resulted in the increased expression of osteogenic markers and enhanced calcification of VICs, underscoring the novel protective role of Cul2 in mitigating VIC calcification under nutrient-restricted conditions *in vitro*. To our knowledge this is the first demonstration of an inhibitory effect of Cul2 on the calcification process, in either a physiological or pathological setting.

While proteomic analysis using SILAC provides valuable mechanistic insights into how NR affects calcification, it should be noted that that glucose serves as the prominent energy source for VICs (36). Indeed, nutrient depletion and manipulation of metabolic substrates may impact the viability, metabolism and contractile behaviour of VICs (37), and warrants investigation in future studies.

Recent studies have also demonstrated that NR also produces a range of negative effects that are not yet fully understood. These include reduced wound healing capacity, increased cold sensitivity, and altered bone health (38). Further studies exploring the *in vivo* effects of NR on CAVD and long-term safety data are therefore now required in relevant animal models such as the murine wire-induced aortic valve stenosis model (39).

Neverltheless, our studies highlight the potential for exploring the use of NR mimetics as a potential approach, with candidate compounds including resveratrol, rapamycin and metformin (40).

Indeed, recent data has demonstrated that the putative NR mimetic metformin exerts protect effects against VIC calcification, however associated changes in the UPS pathway were not examined in this study (41).

Our findings also highlight E3 ubiquitin ligase downstream target proteins as a novel therapeutic strategy against CAVD. These target proteins include APC/CCdh1 which can suppress the MEK/ERK pathway by targeting the senescence inducer BRAF kinase for degradation (42). Additionally, the RBR type E3 ligase Parkin is important in controlling mitochondrial homeostasis and ROS generation (43). As alterations in senescence and mitochondrial function have been recently proposed to drive vascular calcification (44), future exploration of the role of these downstream targets of E3 ubiquitin ligase would be of great interest.

In summary, our study highlights NR as a promising intervention for preventing VIC calcification, with the ubiquitination pathway emerging as a key mediator of this protective effect. The therapeutic potential of proteasome or E3 ligase activators represents a novel avenue for managing calcific aortic stenosis and warrants further investigation.

## Data availability statement

The original contributions presented in the study are included in the article/Supplementary Material, further inquiries can be directed to the corresponding authors.

## Ethics statement

Ethical approval was not required for the studies on animals in accordance with the local legislation and institutional requirements because only commercially available established cell lines were used.

## Author contributions

KP: Data curation, Formal analysis, Investigation, Validation, Writing – original draft, Writing – review & editing, Conceptualization, Methodology, Project administration, Supervision. QT: Writing – original draft, Writing – review & editing. DK: Data curation, Formal analysis, Investigation, Methodology, Software, Validation, Writing – review & editing. XT: Data curation, Formal analysis, Investigation, Methodology, Software, Writing – review & editing. WC: Data curation, Investigation, Supervision, Writing – review & editing. VM: Conceptualization, Funding acquisition, Investigation, Project administration, Resources, Supervision, Writing – review & editing.

## Funding

The author(s) declare that financial support was received for the research and/or publication of this article. This work was supported by funding from the Biotechnology and Biological Sciences Research Council (BBSRC) in the form of an Institute Strategic Programme Grant (BB/J004316/1, BBS/E/D/20221657 and BBS/E/RL/230001C). VEM is a member of the International Network on Ectopic Calcification (INTEC, https://www.itnintec.com). For the purpose of open access, the author has applied a CC-BY public copyright licence to any Author Accepted Manuscript version arising from this submission.

## Conflict of interest

The authors declare that the research was conducted in the absence of any commercial or financial relationships that could be construed as a potential conflict of interest.

The author(s) declared that they were an editorial board member of Frontiers, at the time of submission. This had no impact on the peer review process and the final decision.

## Generative AI statement

The author(s) declare that no Generative AI was used in the creation of this manuscript.

## Publisher's note



## References

1. Carabello BA, Paulus WJ. Aortic stenosis. *Lancet*. (2009) 373(9667):956–66. doi: 10.1016/S0140-6736(09)60211-7

2. Rajamannan NM, Evans FJ, Aikawa E, Grande-Allen KJ, Demer LL, Heistad DD, et al. Calcific aortic valve disease: not simply a degenerative process a review and agenda for research from the national heart and lung and blood institute aortic stenosis working group. *Circulation*. (2011) 124(16):1783. doi: 10.1161/CIRCULATIONAHA.110.006767

3. Jono S, Shioi A, Ikari Y, Nishizawa Y. Vascular calcification in chronic kidney disease. *J Bone Miner Metab*. (2006) 24:176–81. doi: 10.1007/s00774-005-0668-6

4. Nakamura A, Dohi Y, Akahane M, Ohgushi H, Nakajima H, Funaoka H, et al. Osteocalcin secretion as an early marker of *in vitro* osteogenic differentiation of rat mesenchymal stem cells. *Tissue Eng Part C Methods*. (2009) 15(2):169–80. doi: 10.1089/ten.tec.2007.0334

5. Kaden JJ, Bickelhaupt S, Grobholz R, Vahl C, Hagl S, Brueckmann M, et al. Expression of bone sialoprotein and bone morphogenetic protein-2 in calcific aortic stenosis. *J Heart Valve Dis*. (2004) 13(4):560–6.

6. Goldbarg SH, Elmariah S, Miller MA, Fuster V. Insights into degenerative aortic valve disease. *J Am Coll Cardiol*. (2007) 50(13):1205–13. doi: 10.1016/j.jacc.2007.06.024

7. Lerman DA, Prasad S, Alotti N. Calcific aortic valve disease: molecular mechanisms and therapeutic approaches. *Eur Cardiol Rev*. (2015) 10(2):108. doi: 10.15420/ecr.2015.10.2.108

8. Baranowski T, Cullen KW, Baranowski J. Psychosocial correlates of dietary intake: advancing dietary intervention. *Annu Rev Nutr*. (1999) 19(1):17–40. doi: 10.1146/annurev.nutr.19.1.17

9. Brandhorst S, Longo VD. Dietary restrictions and nutrition in the prevention and treatment of cardiovascular disease. *Circ Res*. (2019) 124(6):952–65. doi: 10.1161/CIRCRESAHA.118.313352

10. Dilova I, Easlon E, Lin S-J. Calorie restriction and the nutrient sensing signaling pathways. *Cell Mol Life Sci*. (2007) 64:752–67. doi: 10.1007/s00018-007-6381-y

11. Liu GY, Sabatini DM. mTOR at the nexus of nutrition, growth, ageing and disease. *Nat Rev Mol Cell Biol*. (2020) 21(4):183–203. doi: 10.1038/s41580-019-0199-y

12. Wu Z, Isik M, Moroz N, Steinbaugh MJ, Zhang P, Blackwell TK. Dietary restriction extends lifespan through metabolic regulation of innate immunity. *Cell Metab*. (2019) 29(5):1192–205.e8. doi: 10.1016/j.cmet.2019.02.013

13. Lin C, Zhu D, Markby G, Corcoran BM, Farquharson C, Macrae VE. Isolation and characterization of primary rat valve interstitial cells: a new model to study aortic valve calcification. *J Vis Exp*. (2017) 20(129):56126. doi: 10.3791/56126

14. Rampersad SN. Multiple applications of Alamar blue as an indicator of metabolic function and cellular health in cell viability bioassays. *Sensors*. (2012) 12(9):12347–60. doi: 10.3390/s120912347

15. Tang Q, Markby GR, MacNair AJ, Tang K, Tkacz M, Parys M, et al. TGF-B-induced PI3K/AKT/mTOR pathway controls myofibroblast differentiation and secretory phenotype of valvular interstitial cells through the modulation of cellular senescence in a naturally occurring *in vitro* canine model of myxomatous mitral valve disease. *Cell Prolif*. (2023) 56(6):e13435. doi: 10.1111/cpr.13435

16. Cui L, Rashdan NA, Zhu D, Milne EM, Ajuh P, Milne G, et al. End stage renal disease-induced hypercalcemia may promote aortic valve calcification via annexin VI enrichment of valve interstitial cell derived-matrix vesicles. *J Cell Physiol*. (2017) 232(11):2985–95. doi: 10.1002/jcp.25935

17. Tang Q, Tang K, Markby GR, Parys M, Phadwal K, MacRae VE, et al. Autophagy regulates cellular senescence by mediating the degradation of CDKN1A/p21 and CDKN2A/p16 through SQSTM1/p62-mediated selective autophagy in myxomatous mitral valve degeneration. *Autophagy*. (2025) 21(7):1433–55. doi: 10.1080/15548627.2025.2469315

18. Phadwal K, Koo E, Jones RA, Forsythe RO, Tang K, Tang Q, et al. Metformin protects against vascular calcification through the selective degradation of Runx2 by the p62 autophagy receptor. *J Cell Physiol*. (2022) 237(11):4303–16. doi: 10.1002/jcp.30887

19. Uriarte M, Sen Nkwe N, Tremblay R, Ahmed O, Messmer C, Mashtalir N, et al. Starvation-induced proteasome assemblies in the nucleus link amino acid supply to apoptosis. *Nat Commun*. (2021) 12(1):6984. doi: 10.1038/s41467-021-27306-4

20. Kamura T, Maenaka K, Kotoshiba S, Matsumoto M, Kohda D, Conaway RC, et al. VHL-box and SOCS-box domains determine binding specificity for Cul2-Rbx1 and Cul5-Rbx2 modules of ubiquitin ligases. *Genes Dev*. (2004) 18(24):3055–65. doi: 10.1101/gad.1252404

21. Dorling JL, Martin CK, Redman LM. Calorie restriction for enhanced longevity: the role of novel dietary strategies in the present obesogenic environment. *Ageing Res Rev*. (2020) 64:101038. doi: 10.1016/j.arr.2020.101038

22. Krstic J, Reinisch I, Schindlmaier K, Galhuber M, Riahi Z, Berger N, et al. Fasting improves therapeutic response in hepatocellular carcinoma through p53-dependent metabolic synergism. *Sci Adv*. (2022) 8(3):eabh2635. doi: 10.1126/sciadv.abh2635

23. Li F, Zhang L, Craddock J, Bruce-Keller AJ, Dasuri K, Nguyen A, et al. Aging and dietary restriction effects on ubiquitination, sumoylation, and the proteasome in the heart. *Mech Ageing Dev*. (2008) 129(9):515–21. doi: 10.1016/j.mad.2008.04.007

24. Wang T, Zhang Y, Liu Y, Huang Y, Wang W. Amino acid-starved cancer cells utilize macropinocytosis and ubiquitin-proteasome system for nutrient acquisition. *Advanced Science*. (2024) 11(1):2304791. doi: 10.1002/advs.202304791

25. Feng J, Li Y, Zhang Y, Sun S, Sun J, Xu Q, et al. Endothelium-specific deletion of p62 causes organ fibrosis and cardiac dysfunction. *J Transl Med*. (2024) 22(1):161. doi: 10.1186/s12967-024-04946-w

26. Daren L, Dan Y, Jinhong W, Chao L. NIK-mediated reactivation of SIX2 enhanced the CSC-like traits of hepatocellular carcinoma cells through suppressing ubiquitin–proteasome system. *Environ Toxicol*. (2024) 39(2):583–91. doi: 10.1002/tox.23892

27. Komander D, Rape M. The ubiquitin code. *Annu Rev Biochem*. (2012) 81:203–29. doi: 10.1146/annurev-biochem-060310-170328

28. Kaushik S, Cuervo AM. Proteostasis and aging. *Nat Med*. (2015) 21(12):1406–15. doi: 10.1038/nm.4001

29. Hiam-Galvez KJ, Allen BM, Spitzer MH. Systemic immunity in cancer. *Nat Rev Cancer*. (2021) 21(6):345–59. doi: 10.1038/s41568-021-00347-z

30. Saitoh H, Hinchey J. Functional heterogeneity of small ubiquitin-related protein modifiers SUMO-1 versus SUMO-2/3*. *J Biol Chem*. (2000) 275(9):6252–8. doi: 10.1074/jbc.275.9.6252

31. Afsar M, Liu G, Jia L, Ruben EA, Nayak D, Sayyad Z, et al. Cryo-EM structures of Uba7 reveal the molecular basis for ISG15 activation and E1-E2 thioester transfer. *Nat Commun*. (2023) 14(1):4786. doi: 10.1038/s41467-023-39780-z

32. Cai Z, Ding Y, Zhang M, Lu Q, Wu S, Zhu H, et al. Ablation of adenosine monophosphate-activated protein kinase $\alpha$1 in vascular smooth muscle cells promotes diet-induced atherosclerotic calcification *in vivo*. *Circ Res*. (2016) 119(3):422–33. doi: 10.1161/CIRCRESAHA.116.308301

33. Kwon DH, Shin S, Nam YS, Choe N, Lim Y, Jeong A, et al. CBL-b E3 ligase-mediated neddylation and activation of PARP-1 induce vascular calcification. *Exp Mol Med*. (2024) 56(10):2246–59. doi: 10.1038/s12276-024-01322-y

34. Lim KH, Joo JY. Predictive potential of circulating Ube2h mRNA as an E2 ubiquitin-conjugating enzyme for diagnosis or treatment of Alzheimer's disease. *Int J Mol Sci*. (2020) 21(9):3398. doi: 10.3390/ijms21093398

35. Cai W, Yang H. The structure and regulation of Cullin 2 based E3 ubiquitin ligases and their biological functions. *Cell Div*. (2016) 11:7. doi: 10.1186/s13008-016-0020-7

36. Sánchez-Bayuela T, Peral-Rodrigo M, Parra-Izquierdo I, López J, Gómez C, Montero O, et al. Inflammation via JAK-STAT/HIF-1$\alpha$ drives metabolic changes in pentose phosphate pathway and glycolysis that support aortic valve cell calcification. *Arterioscler Thromb Vasc Biol*. (2025) 45(7):e232–49. doi: 10.1161/ATVBAHA.124.322375

37. Kamel PI, Qu X, Geiszler AM, Nagrath D, Harmancey R, Taegtmeyer H, et al. Metabolic regulation of collagen gel contraction by porcine aortic valvular interstitial cells. *J R Soc Interface*. (2014) 11(101):20140852. doi: 10.1098/rsif.2014.0852

38. Wang A, Speakman JR. Potential downsides of calorie restriction. *Nat Rev Endocrinol*. (2025) 21(7):427–40. doi: 10.1038/s41574-025-01111-1

39. Niepmann ST, Steffen E, Zietzer A, Adam M, Nordsiek J, Gyamfi-Poku I, et al. Graded murine wire-induced aortic valve stenosis model mimics human functional and morphological disease phenotype. *Clin Res Cardiol*. (2019) 108:847–56. doi: 10.1007/s00392-019-01413-1

40. Madeo F, Carmona-Gutierrez D, Hofer SJ, Kroemer G. Caloric restriction mimetics against age-associated disease: targets, mechanisms, and therapeutic potential. *Cell Metab*. (2019) 29(3):592–610. doi: 10.1016/j.cmet.2019.01.018

41. Phadwal K, Tan X, Koo E, Zhu D, MacRae V. Metformin ameliorates valve interstitial cell calcification by promoting autophagic flux. *Sci Rep*. (2023) 13(1):21435. doi: 10.1038/s41598-023-47774-6

42. Wan L, Chen M, Cao J, Dai X, Yin Q, Zhang J, et al. The APC/C E3 ligase complex activator FZR1 restricts BRAF oncogenic function. *Cancer Discov*. (2017) 7(4):424–41. doi: 10.1158/2159-8290.CD-16-0647

43. Pickrell AM, Youle RJ. The roles of PINK1, parkin, and mitochondrial fidelity in Parkinson's disease. *Neuron*. (2015) 85(2):257–73. doi: 10.1016/j.neuron.2014.12.007

44. Phadwal K, Tang Q-Y, Luijten I, Zhao J-F, Corcoran B, Semple RK, et al. P53 regulates mitochondrial dynamics in vascular smooth muscle cell calcification. *Int J Mol Sci*. (2023) 24(2):1643. doi: 10.3390/ijms24021643